

Assessment of Submarine Landslide Volume

Thore Falk Sager (✉ tsager@geomar.de)

GEOMAR Helmholtz Centre for Ocean Research Kiel

Morelia Urlaub

GEOMAR Helmholtz Centre for Ocean Research Kiel

Christian Berndt

GEOMAR Helmholtz Centre for Ocean Research Kiel

Research Article

Keywords: volume assessment, pre-failure seafloor reconstruction, landslide volume, emplacement mechanism

Posted Date: August 16th, 2023

DOI: <https://doi.org/10.21203/rs.3.rs-3205387/v1>

License:   This work is licensed under a Creative Commons Attribution 4.0 International License.

[Read Full License](#)

Abstract

Submarine landslides pose major geohazards as they can destroy seafloor infrastructure such as communication cables and cause tsunamis. The volume of material displaced with the landslide is one factor that determines its hazard and is typically estimated using bathymetric and/or seismic datasets. Here, we review methods to determine the initial failed volume based on a well-constrained case study, the Ana Slide, a small slope failure in the Eivissa Channel off the eastern Iberian Peninsula. We find that not only the availability and quality of datasets but also the emplacement mechanism determines the quality of the volume estimation. In general, the volume estimation based on comparison of modern and reconstructed pre-failure seafloor topographies yields conservative, yet robust volumes for the amount of material that was mobilized. In contrast, volume estimated from seismic data may be prone to overestimation if no detailed constraints on the nature of the chaotic, transparent, or disrupted seismic facies commonly used to identify landslide material are available.

1. Introduction

Submarine landslides are a serious geohazard to coastal populations worldwide (Bondevik et al., 2005; Haugen et al., 2005; Løvholt et al., 2017; Prior et al., 1984; Synolakis et al., 2002; P. Talling et al., 2014; Watt et al., 2012). Slope failures can destroy offshore infrastructure such as platforms and telecommunication cables (e.g., Løvholt et al., 2019; Vanneste et al., 2014) and release large quantities of methane and other greenhouse gases from the seafloor (e.g., Maslin et al., 2004). While the record of slope failure-generated tsunamis is mainly limited to their deposits on land (e.g., Bondevik et al., 1997, 2005; Fruergaard et al., 2015), mass-transport deposits (MTDs) are widespread features on the ocean floor (e.g., Camerlenghi et al., 2010; Gatter et al., 2021; Moscardelli & Wood, 2015). The inclination of the seafloor, water depth, duration of the slide event, its acceleration, related landslide mechanisms, run-out velocity, the timing between multiple stages of failure, the volume of mobilized material, and its density and cohesion are all factors that control the impact of a landslide (e.g., Harbitz et al., 2014; Murty, 2003). Constraining these factors requires seafloor samples and age datings that are rarely available. Some factors, such as the acceleration and propagation velocity cannot be quantified at all from MTDs. While the landslide mechanism is one of the most important factors for the generation of tsunamis (e.g., Synolakis et al., 2002), this is also difficult to quantify. However, the volume of a submarine landslide can be estimated relatively easily from bathymetry and/or a few seismic lines. The volume of a landslide is not constant as it may change during the evolution of the landslide. The volume of the deposit may thus exceed the initial failed volume because of processes like basal erosion and entrainment (e.g., Sobiesiak et al., 2018; Watt et al., 2012). On the other hand, the deposit may be distributed over large areas by highly mobile sediment flows (P. J. Talling et al., 2007), which can escape the resolution of mapping and imaging systems. Here, we focus particularly on the initial failed volume of a landslide as it is one of the key input parameters for tsunami models (e.g., Iglesias et al., 2012; Murty, 2003).

There are various ways to estimate the volume of submarine landslides from bathymetric or reflection seismic data. McAdoo et al. (2000) measured the area of the source area (A) and height of the headscarp

(H) from bathymetric data to estimate the evacuated volume through $\text{volume} = 1/2 * A * H$. On the contrary, Völker (2010) estimated the evacuated volume by subtracting a pre-failure seafloor that was reconstructed by fitting slope functions into the landslide scar from the present-day seafloor. Here, a negative volume in the source area provides an estimate of the initial failed volume and a positive volume in the sink area provides an estimate of the deposited and accumulated volume. Wilson et al. (2004) calculated the volume of a debris lobe from measures of its depth or thickness (D), width (W), and length (L) through the relationship of $\text{volume} = 1/6 * \pi * D * W * L$. For landslides that are imaged from sub-seafloor sediment echo-sounder profiles or 2D and 3D reflection seismic data, the average thickness of chaotic, transparent, and disrupted seismic facies representing the mobilized material can be measured and multiplied by the landslide area. This provides the 'bulk volume' of material involved in and affected by the landslide referred to as Vd by Nugraha et al. (2022) that accumulated inside the sink area. This method was used by Lastras et al. (2004) to estimate the landslide volume or total affected volume of Ana Slide, located in the Eivissa Channel, western Mediterranean Sea. These authors used the average thickness of Ana Slide at 23 m inside the landslide scar (with an area of 6 km²) to propose a volume or Vd (sensu Nugraha et al., 2022) of 0.14 km³.

This study aims to determine the most suitable and robust approach to determine this initial failed volume, in particular in the absence of extensive coverage of reflection seismic data and geological sampling. This is done for the Ana Slide in the Eivissa Channel located in the western Mediterranean Sea, for which the landslide structure, as well as the development, emplacement, evacuation, and accumulation processes, are known in the much detail. Ana Slide is entirely covered by high-resolution 3D reflection seismic data. Both the detailed knowledge and complete coverage of seismic data allow us to determine its volume with low uncertainties.

2. Emplacement of Ana Slide

Ana Slide is a relatively small landslide located on the eastern slopes of the Eivissa Channel, western Mediterranean Sea between 635 and 790 m water depth (Berndt et al., 2012; Lastras et al., 2004, 2006; Sager et al., 2022) (Fig. 1b). Beneath Ana Slide the pre-Ana Slide was previously identified by Lastras et al. (2004) and mapped by Berndt et al. (2012) and Sager et al. (2022) with a congruent headscarp toward the east while the pre-Ana Slide extends around 1.5 km further toward the west (Fig. 1b). We take the interpretation of development and emplacement processes of Ana Slide presented by Sager et al. (2022). These authors use high-resolution bathymetry, 3D reflection seismic data and re-processed 2D reflection seismic profiles that completely cover this landslide. Sager et al. (2022) show that Ana Slide developed during two stages referred to as the primary (300 ka) and secondary failures (61.5 ka after Cattaneo et al., 2011). The primary failure involved slope material located between the basal shear surface represented by the reference reflector Ref and the sub-reflector R1 (Sager et al., 2022) (Fig. 2a and b). The landslide material emerged frontally, travelled across a 500 m long by-pass zone, and accumulated above the pre-failure seafloor at the time of the primary failure represented by the 'pre-failure R1 reflector' inside the sink area as the 'actual deposit of the primary failure' (Fig. 2a and b). The accumulation of this deposit

induced in situ deformation of the underlying sediments reaching a depth of up to 30 m below the pre-failure R1 reflector throughout the sink area that marked the seafloor during the primary failure (Fig. 2f). Landslide material mobilized during the primary failure accumulated inside the sink area and attained a thickness of approximately 15 m. The secondary failure involved slope material between R1 and SFR. It was much smaller and is not seismically resolved even in high-resolution seismic data (~ 5 m vertical resolution, Berndt et al., 2012).

For this study, the primary and secondary failures of Ana Slide are combined as the seismic data do not allow to distinguish the secondary failure deposit from the seafloor reflection (Fig. 2b). Consequently, the top reflector of Ana Slide referred to as SFR corresponds to the occurrence of the secondary failure.

Submarine landslides can generally be defined as those that are frontally confined or frontally emergent (Frey Martinez et al., 2006). A confined landslide experiences restricted downslope translation above a basal shear surface at depth and it is unable to emerge frontally onto the seafloor, whereas an unconfined landslide can emerge frontally onto the seafloor and propagate freely above the seafloor leaving the source area entirely evacuated. On the one hand side landslide material is mobilized and evacuated from a source area where it leaves a void space between the pre-failure and present-day seafloor. On the other hand, this landslide material accumulates inside the sink area and if the landslide is frontally emergent this landslide material may propagate further downslope as a turbidity current and lay down a debris flow or turbidite deposit over a large area (e.g., Lastras et al., 2002). Ana Slide describes a mixed system landslide. The primary failure developed as frontally emergent while the secondary failure developed more like a frontally confined slope failure. A fraction of the mobilized landslide material was able to overcome frontal confinement and emerge onto the seafloor. The other part of the mobilized material remained ponded inside the source area defined as 'undifferentiated landslide material' by Sager et al. (2022) (Fig. 2b).

2.1. Tectonic setting of the Ana Slide area

Sager et al. (2022) and Berndt et al. (2012) identified several faults inside the extent of the 3D reflection seismic data (Fig. 1b). Three of these, the southern, central, and northern faults are located beneath the sink area of Ana Slide and further south of it. These faults characterize an en-echelon fault system that strikes SSW and NNE and extends into the 3D reflection seismic data from the south with an unknown extent. This fault system dips in the opposite direction compared to the seafloor and therefore is termed 'seafloor antithetic' in this study. Primarily the northern but also the central fault affected the seafloor morphology before the primary failure of Ana Slide by vertical fault movement (Sager et al., 2022).

2.2. Depositional environment in the Eivissa Channel

Eivissa Channel received a limited input of terrestrial sediments from rivers on the Iberian Peninsula including the Ebro, Turia, and Jucar and there are no permanent rivers on the Balearic Islands (Lafuerza et al., 2012; Lastras et al., 2004; Panieri et al., 2012). Steady hemipelagic sedimentation with the deposition of fine-grained water-rich marine clays enriched in calcareous nano fossils generated well-stratified

seafloor sub-parallel reflectors and there exists no evidence for strong bottom currents or contourites (e.g., Lastras et al., 2004). In profile, the thickness of the interval between reflector Ref and SFR increases in the downslope direction toward the west with increasing water depth (Sager et al., 2022 their Fig. 4c) generating predictable thicknesses of these stratigraphic intervals.

3. Datasets

This study uses bathymetric data and 3D reflection seismic data acquired with the P-Cable system of the National Oceanographic Centre (NOC) in Southampton, UK equipped with two sleeve guns and 11 streamers during cruise 178 onboard RSS Charles Darwin in 2006 (CD178). Data were processed including time migration with water velocity (1500 m s^{-1}). For further information about acquisition and processing workflows, the reader is referred to Berndt et al. (2012) and Sager et al. (2022). The bathymetric data have a horizontal resolution of 5 m, and the vertical resolution is approximately 0.5% of the water depth (Fig. 1b) while the 3D reflection seismic data have a vertical resolution of 5–6 m and a horizontal resolution of 10–15 m (Berndt et al., 2012). The 2D reflection seismic profile presented in Fig. 2a shows a re-processed profile presented previously by Sager et al. (2022).

4. Methods for volume estimation of submarine landslides through pre-failure seafloor reconstructions

Volume calculations of evacuated and accumulated landslide material of Ana Slide are performed in Kingdom Suite using the Volumetric tool that uses one bounding polygon and two depth-converted grids in meters depth (calculated from horizons in seconds two-way travel time or seconds TWTT). For depth conversion of seismic horizons, a seismic velocity of 1500 m s^{-1} is used. This velocity is consistent with seismic velocity measurements from the shallow 8 m long Kullenberg gravity core PSM-KS18 ($0^\circ 50.453' \text{ E } 38^\circ 38.184' \text{ N}$) presented by Lafuerza et al. (2012) obtained during the PRISM cruise with the R/V *L'Atalante* in 2007 led by IFREMER, France. The 3D reflection seismic data are presented in the time domain (seconds TWTT) and volumes are calculated in the upper 50 m beneath the seafloor. Sediments are water-rich (Lafuerza et al., 2012; Lastras et al., 2004; Panieri et al., 2012) and seismic P-wave velocities of such sediments typically vary between 1500 to 1640 m s^{-1} (Hamilton, 1979). Thus, a seismic velocity of 1500 m s^{-1} is appropriate to use for depth conversion of seismic reflectors Ref and SFR and the reconstructed pre-failure seafloors for the source and sink areas.

In this study, three horizontal bounding polygons are defined: the source area that covers an area of 1.9 km^2 , the by-pass zone with an area of 0.45 km^2 , and the sink area covering an area of 2.45 km^2 (Figs. 1b and 2c). In total, Ana Slide covers an area of 4.8 km^2 referred to as the landslide scar.

We define several landslide volumes (Figs. 2 and 3), the values of which are calculated independently and with different approaches:

Apparent evacuated volume ($V_{e \text{ void}}$)

the void space in the source area. $V_{e_{void}}$ is calculated following the approach of Völker (2010) where the volume of evacuated landslide material is calculated by comparing the present-day with the reconstructed pre-failure seafloors (e.g, Omira et al., 2022; Sun et al., 2018; Webster et al., 2016). The pre-failure seafloor of the source area of Ana Slide is reconstructed by manually interpolating the course of local and regional contour lines from outside the landslide scar into the inside of it using the contour-line approach (Fig. 2a and b). To test the sensitivity of the applied pre-failure seafloor reconstructions, we reconstructed the seafloor inside the source area assuming a simple yet unlikely realistic pre-failure seafloor morphology (referred to as the straight-line approach hereafter). This was done by reconstructing straight pre-failure contour lines between the intersection of the landslide scar with local 10 m contour lines (Figure S1). The resulting calculated volume of evacuated landslide material from the source area serves as the maximum value for $V_{e_{void}}$.

Remaining volume (V_{e_r})

the volume of 'undifferentiated landslide material' (sensu Sager et al., 2022) that remained inside and was mobilized but did not leave the source area of Ana Slide. It is calculated from the 3D reflection seismic data and represents the difference between the present-day seafloor (SFR) and the basal shear surface (Ref) in the source area.

Turbidite volume (V_t)

the volume of material which potentially was transported into the deeper basin and out of the study area by turbidity currents. This material accumulated over a potentially vast area approaching zero thickness. With the available geophysical datasets limited to the proximal area of Ana Slide, it is impossible to determine whether a turbidity current was caused nor to estimate the volume of the turbidite deposit because of the lack of appropriate distal geological sampling. In the following, we, therefore, assume $V_t = 0$ for Ana Slide.

Evacuated volume (V_e)

the initial failed volume. It is the sum of $V_{e_{void}}$, V_{e_r} , and V_t (if a turbidite deposit was generated in the distal part):

$$V_e = V_{e_{void}} + V_{e_r} + V_t.$$

Bulk accumulated volume ($V_{a_{bulk}}$)

chaotic, transparent, and disrupted seismic facies representing mobilized and affected landslide material and slope sediment. This volume is calculated from 3D reflection seismic data between the present-day seafloor and reflector Ref in the sink area. This volume is referred to as volume deposited V_d by Nugraha et al. (2022).

Accumulated volume (V_a)

the amount of material that accumulated above the pre-failure seafloor and the present-day seafloor SFR inside the sink area. It represents the difference between the apparent evacuated volume of $V_{e_{void}}$ and the volume of a potential turbidite deposit and therefore:

$$V_a = V_{e_{void}} - V_t.$$

The approach of Völker (2010) could be used to estimate V_a . However, for Ana Slide, the morphology of the sink area was modified by a local seafloor antithetic en-echelon fault system before the failure occurred and before the primary failure (Sager et al., 2022). Thus, the pre-failure seafloor inside the sink area cannot be reconstructed using the contour-line approach previously used for the source area. Therefore, to account for vertical fault movement in the pre-failure seafloor reconstruction, the predictable thickness of sedimentary sequences (between Ref and SFR) throughout the study area is used to constrain the course of the pre-failure seafloor inside the sink area (Fig. 2b and e). For the horizon-flattening approach, first reflectors Ref and SFR are picked in the 3D reflection seismic data. Then, reflector SFR is removed from inside the sink area. For pre-failure seafloor reconstruction, reflector Ref is horizontally flattened and SFR is reconstructed inside the sink area using the predictable thickness of the stratigraphic sequence between reflectors Ref and SFR by manually picking straight lines that represent this thickness between the upslope and downslope extent of the source area on individual inlines (the workflow is presented in Figure S2). After reconstruction is completed, reflector Ref is de-flattened with the resulting reconstructed pre-failure seafloor accounting for vertical tectonic movement of the seafloor antithetic en-echelon fault system with activity before failure occurrence of the primary failure of Ana Slide (Sager et al., 2022). The resulting surface is called the 'pre-failure seafloor following the horizon-flattening approach' (Fig. 2b and e).

4.1. Uncertainties of volume estimations

General uncertainties for volume estimation are related to reflection seismic data such as unknown seismic velocities, lateral changes in seismic velocities, and reflector picking errors (related to the vertical seismic resolution). Additional uncertainties unique to Ana Slide are related to the localization of bounding polygons of the source and sink areas related to the horizontal resolution of reflection seismic data and those related to issues with ghost artefacts in the 3D reflection seismic data previously discussed by Sager et al. (2022). Overall, the picking errors are small for 3D reflection seismic data (< 5% of the total volume) and the uncertainty due to unknown seismic velocity is small for the uppermost sediments (< 5%), while the uncertainty related to polygons of the source and sink areas is neglectable (< 2%).

Dugan (2012) and Sun & Alves (2020) demonstrate that MTD material has higher density and lower porosity compared to background sediment, which would impact the seismic velocity of the landslide interval. A comparison of several cores inside and outside the landslide area shows that no notable

differences in P-wave velocities in background sediment and MTD exist, at least in the upper 8 m (Lafuerza et al., 2012). Therefore, we assume no uncertainties resulting from lateral variations in seismic velocities.

The above uncertainties affect the different volume estimations in distinct ways. In sum, the above uncertainties of the volume estimation of Ana Slide add up to 12%. Uncertainties related to the approach to pre-failure seafloor reconstruction are significantly larger but difficult to quantify in percentages (Table 1).

Volume assessment of Ana Slide assumes that slope failure occurred at once. From the analysis of the development and emplacement processes of Ana Slide (Sager et al., 2022), it is known that it developed during two overall stages of failure separated by around 240 ka. Because of limited vertical seismic resolution (5 m), it is not possible to identify the boundary between the two, which would be needed to differentiate between the individual volumes. Hence, despite better knowledge, we have to consider both as one and therefore V_e given here overestimates the initial failed volume for the main (primary) failure.

Table 1

Results from volume assessment of Ana Slide. Names of volumes calculated, and bounding surfaces are presented. The volume of $V_{e_{void}}$ (evacuated volume from the source area) and V_a (volume accumulated above the pre-failure seafloor inside the sink area) is the same at 0.016 km^3 (b and d).

Name	Upper surface (depth-converted horizons)	Lower surface (depth-converted horizons)	Bounding polygon	Areal extent (km^2)	Volume (km^3)
a V_{e_r}	present-day seafloor (SFR)	reference reflector (Ref)	source area	1.90	0.024
b $V_{e_{void}}$	reconstructed pre-failure seafloor using the contour-line approach	present-day seafloor (SFR)	source area	1.90	0.016
Ve	$V_{e_r} + V_{e_{void}}$				0.040
	$V_{e_r} + V_a$				0.040
c $V_{a_{bulk}}$	present-day seafloor (SFR)	reference reflector (Ref)	sink area	2.45	0.084
d V_a	present-day seafloor (SFR)	reconstructed pre-failure seafloor using the horizon-flattening approach	sink area	2.45	0.016
e $V_{e_{void}}$ (straight-line approach)	reconstructed pre-failure seafloor using the straight-line approach	present-day seafloor (SFR)	source area	1.90	0.027
f V_a (straight-line approach)	present-day seafloor (SFR)	reconstructed pre-failure seafloor using the straight-line approach	sink area	2.45	0.006

5. Results from volume assessment of Ana Slide

The amount of evacuated landslide material that remained inside the source area of Ana Slide called V_{e_r} is 0.024 km^3 (Table 1a). Together with the volume of $V_{e_{void}}$ of 0.016 km^3 (Table 1b), the amount of all mobilized and involved landslide material from inside the source area called V_e is calculated by:

$$V_e = V_{e_r} + V_{e_{void}} + (V_t), \text{ thus } 0.024 \text{ km}^3 + 0.016 \text{ km}^3 = 0.040 \text{ km}^3 \text{ (Table 1b and d).}$$

The amount of material that was transported and deposited as a turbidite V_t could not be determined and is assumed to be zero.

The amount of apparent bulk landslide material inside the sink area $V_{a_{bulk}}$ is 0.084 km^3 (Table 1c). This volume refers to both the amount of actually accumulated landslide material V_a of 0.016 km^3 above the pre-failure seafloor reconstructed using the horizon-flattening approach (Table 1d), and the slope sediment deformed in situ between the reconstructed seafloor using the horizon-flattening approach and reflector Ref inside the sink area. V_a corresponds to $V_{e_{void}}$ through (V_t is assumed to be zero):

$V_a = V_{e_{void}} - V_t$, thus $0.016 \text{ km}^3 = 0.016 \text{ km}^3$, and therefore $V_a = V_{e_{void}}$ for Ana Slide.

From the simple yet unrealistic pre-failure seafloor reconstruction using the straight-line approach applied inside the landslide scar of Ana Slide, we have estimated the amounts of $V_{e_{void}}$ (straight-line approach) between the reconstructed and present-day seafloors inside the source area at 0.027 km^3 (Table 1e). The amount of V_a estimated between the pre-failure seafloor using the straight-line approach for pre-failure seafloor reconstruction and the present-day seafloor inside the sink area yields a volume of 0.006 km^3 for V_a (Table 1f).

6. Discussion

6.1. Ana Slide volume assessment

The initial failed volume of Ana Slide V_e is the sum of the actually evacuated volume $V_{e_{void}}$ from the source area and the volume of the remaining material V_{e_r} inside the source area (Fig. 3a). Furthermore, V_e can also be expressed as the sum of $V_{e_{void}}$ and the volume of accumulated landslide material in the sink area V_a . For Ana Slide both approaches result in V_e of 0.040 km^3 and thus are consistent (Table 1). This suggests that the Ana Slide did not generate a turbidity current, because otherwise V_e estimated from $V_{e_{void}}$ and V_{e_r} should exceed the V_e estimated from V_a and V_{e_r} .

The volume of $V_{a_{bulk}}$ at 0.084 km^3 (Table 1c) is more than twice as large as V_e . Because of the previously detailed investigations for Ana Slide by Sager et al. (2022), we know the reason for this discrepancy. The deposit of Ana Slide induced in situ deformation that penetrated to a depth of reflector Ref in the sink area so that this deformed slope sediment appears chaotic, transparent, or disrupted in the reflection seismic data. However, the sediment beneath the deposit inside the sink area is not related to the initial failed volume mobilized from the source area V_e as the sediment deformed in situ and only very limited displacement or transport occurred above reflector Ref inside the sink area of Ana Slide (sensu Lastras et al., 2004). Hence, volume estimation based on seismic data considering seismically chaotic facies without further constraints on its origin would overestimate the initial failed volume of Ana Slide by more than 200%.

To obtain the initial failed volume V_e , V_{e_r} and either $V_{e_{void}}$ or V_a need to be known. While $V_{e_{void}}$ (and V_a) can be estimated from bathymetry data alone, for example through comparing the modern and pre-failure seafloors, V_{e_r} can only be identified and quantified using sub-seafloor reflection seismic data. If no

reflection seismic data had been available for Ana Slide, only $V_{e_{\text{void}}}$ could have been estimated. This would have underestimated the initial failed volume by 40% (because $V_e = 0.040 \text{ km}^3$ while $V_{e_{\text{void}}} = 0.016 \text{ km}^3$).

The value of $V_{e_{\text{void}}}$ using the straight-line approach represents the upper limit of $V_{e_{\text{void}}}$ because more realistic pre-failure seafloor reconstructions will estimate a smaller volume of $V_{e_{\text{void}}}$, and contour lines will diverge further upslope following the local and regional trends (Fig. 1b and S1). The maximum $V_{e_{\text{void}}}$ is thus 0.027 km^3 , which exceeds the actual value of $V_{e_{\text{void}}}$ of 0.016 km^3 by far. Similarly, the amount of V_a estimated using the straight-line approach represents the lower limit of V_a because more realistic contour lines will again diverge further upslope than those reconstructed with this approach. This value is much lower than V_a estimated from the 'realistic' seafloor reconstruction.

Ana Slide is known to have formed during two stages of failure (Sager et al., 2022). The volume of the secondary failure is ignored because the thickness of accumulated landslide material is below the vertical seismic resolution. Nevertheless, the potential volume of a deposit resulting from the secondary failure that uniformly covers the entire sink area assuming a thickness of 4 m which is just below the vertical seismic resolution of 5 m would have a volume of $< 0.010 \text{ km}^3$, hence about a fourth of the volume of V_e at 0.040 km^3 (Table 1).

6.2. Volume assessment of unconfined and confined submarine landslides

In this section, we generalize our findings for Ana Slide. For the discussion, it is useful to categorize submarine landslides according to their emplacement mechanisms. Here, we distinguish between two endmembers following the terminology and definition by Frey Martinez et al. (2006) – confined and unconfined types.

In the completely unconfined case, the source area is fully evacuated and devoid of landslide material, therefore $V_e = V_{e_{\text{void}}}$ (Fig. 3b). This is because once a failure emerges frontally, the source area gets evacuated as the failing parts accelerate and gain kinetic energy that creates an uninterrupted process of frontal emergence. V_e can also be estimated by adding V_a and V_t . Consequently, to assess the volume of unconfined submarine landslides, bathymetric data are ideal to estimate the volumes of $V_{e_{\text{void}}}$ (and potentially V_a) by comparing the modern and pre-failure seafloor topographies. Here, any post-slide modifications of the seafloor by external factors, such as tectonic movement or bottom currents, need to be excluded. The bathymetry-based approach will yield more robust values for V_e than approaches based on single profiles of sub-seafloor reflection seismic data. First, it is possible to cover the entire landslide area. Second, estimates for V_e and V_a can be made and compared for additional quality control assuming that $V_e = V_a$, here called volume balance between the source and sink areas and under this assumption, V_a should not exceed V_e . Third, when using sub-seafloor reflection seismic data, a potential flaw could be introduced by estimating $V_{a_{\text{bulk}}}$ instead of V_a . This is because the internals of a submarine landslide may be imaged as chaotic, disrupted, or transparent seismic facies. Sediments that were

disturbed through internal deformation for example by rapid loading (e.g., Sager et al., 2022) or shearing induced by passing landslide material (e.g., Sobiesiak et al., 2018) also display as chaotic, disrupted, or transparent seismic facies. Hence, seismic facies of V_a and $V_{a_{bulk}}$ are similar if not identical and therefore it is difficult if not impossible to distinguish material that moved, was translated, or was deformed in situ. This is problematic because $V_{a_{bulk}}$ may largely exceed V_e (and V_a).

In the case of a confined landslide (Fig. 3c), the initial failed volume of V_e equals the sum of $V_{e_{void}}$ and V_{e_r} , where $V_{e_r} \gg V_{e_{void}}$. In this case, it is impossible to differentiate between V_{e_r} and V_a . The amount of V_{e_r} can be calculated between the present-day seafloor and the basal shear surface and thus this approach requires sub-seafloor reflection seismic data. Using only bathymetric data to determine $V_{e_{void}}$ will underestimate the initial failed volume by the value of V_{e_r} ($V_e = V_{e_{void}} + V_{e_r}$). In the analysis of reflection seismic data, care must be taken in the identification of the basal shear surface. There is a risk to end up estimating $V_{a_{bulk}}$ instead of V_a because of the reasons outlined above.

6.3. How to determine the initial failed volume of submarine landslides?

Based on the above considerations we here provide a framework and recommendations for assessing the initial failed volume of submarine landslides taking into account available datasets and emplacement mechanism (Fig. 4). The framework applies only to landslide scars outcropping at the seafloor in areas, which have not experienced modification of the seafloor since the occurrence of the landslide. Hence, vertical tectonic movement, deposition by sediment transport processes, or ocean currents must be excluded, or these influences need to be accounted for in the pre-failure seafloor reconstruction. For instance, this is demonstrated by the horizon-flattening approach applied for pre-failure seafloor reconstruction performed inside the sink area of Ana Slide.

First, the pre-failure seafloor must be reconstructed using bathymetric data. Then, this reconstructed pre-failure seafloor may act as the upper surface in calculating $V_{e_{void}}$ inside the source area using the present-day seafloor as the lower surface. V_a is calculated between the present-day and reconstructed pre-failure seafloor inside the sink area. Now, the suggested workflow deviates according to the emplacement mode (unconfined or confined).

In the case the given submarine landslide developed as frontally unconfined (left branch in Fig. 4), it is beneficial to have seismic data covering the source area so that the amount of remaining landslide material (V_{e_r}) can be calculated in order to estimate the complete initial failed volume by $V_e = V_{e_{void}} + V_{e_r}$. V_e can also be estimated from $V_e = V_a + V_t$. In the case no reflection seismic data are available, the rule that $V_{e_{void}} \geq V_a$ can serve as an additional constraint. V_a cannot be larger than $V_{e_{void}}$ because the material deposited in the sink area (estimated based on bathymetry) cannot exceed what was evacuated from the source area while V_a can decrease if landslide material is transported as a turbidity current (V_t). If this condition, nevertheless, is not fulfilled one should revise the pre-failure seafloor reconstruction until the condition is fulfilled. In both cases, if reflection seismic data are available or not, it is robust to

calculate $V_{e_{void}}$ inside the sink area, because it either represents the amount of initial failed landslide material and represents the amount of V_a , or the pre-failure seafloor reconstruction is incorrect assuming that no turbidite transported landslide material (not resolvable in the bathymetric data) and that no erosion and incorporation of seafloor sediment occurred.

In the case the given submarine landslide developed as frontally confined (right branch in Fig. 4) if reflection seismic data are available, the amount of all landslide material involved in or affected by the slope failure can be calculated as the bulk accumulated volume $V_{a_{bulk}}$. For frontally confined submarine landslides the amount of $V_{a_{bulk}}$ is equal to V_e only in the case where no deep deformation has occurred. In that case, $V_{a_{bulk}}$ is larger than V_e . $V_{e_{void}}$ underestimates V_e because the source area is only partly evacuated. In case no sub-seafloor reflection seismic data is available, the only means to approximate the initial failed volume of a submarine landslide is by $V_{e_{void}}$ and V_a , both of which will underestimate V_e .

In case the given landslide developed as a mixed system placed kinematically between the unconfined and confined case, or if the emplacement mode is unknown, we suggest estimating $V_{e_{void}}$ and V_a . If the amount of landslide material transported and deposited as a turbidite is neglectable, the amount of $V_{e_{void}}$ and V_a should be the same ($V_{e_{void}} = V_a$). If V_{e_r} is unknown, one should consider that $V_{e_{void}}$ and V_a likely underestimate V_e by the unknown amount of V_{e_r} .

We showed that for Ana Slide, $V_{a_{bulk}}$ based on seismic data overestimates V_e by more than 200% whereas estimating V_e from $V_{e_{void}}$ and/or V_a based on bathymetry data alone underestimates V_e by 40%. Due to the risk of excessive overestimation, we suggest that the $V_e = V_{e_{void}} + V_{e_r}$ approach should always be preferred over the $V_{a_{bulk}}$ approach, even if V_{e_r} is unknown.

6.4. Limitations and assumption of submarine landslide volume assessments

Estimation of V_e relies on the approach to pre-failure seafloor reconstruction. This may be challenging for submarine landslides in morphologically complex settings and pre-failure seafloor reconstruction might require a certain degree of subjectivity. For instance, the seafloor morphology of the source area before the failure of Ana Slide may have been influenced by the earlier pre-Ana Slide source area (Berndt et al., 2012; Sager et al., 2022). It is clear that V_e and $V_{e_{void}}$ must be equal or larger than V_a (if $V_t > \text{zero}$). This constraint can help assess the quality of the seafloor reconstruction at least in one direction.

Volume estimation based on bathymetry and pre-failure seafloor reconstructions also relies on the assumption that the seafloor has not changed significantly since the occurrence of the landslide. Any modifications of the seafloor, for instance by vertical tectonic movements, erosion, deposition by sediment transport, or ocean currents will result in wrong volume estimates. Another assumption is that the volume has been evacuated during one event. If the volume was evacuated during multiple stages with significant time gaps in between, for instance, the potential hazard will likely be overestimated,

although controlled by many other factors such as landslide mechanisms, angle of the slide, water depth, density and cohesion of the landslide material, duration of the slide event, its acceleration, and run-out velocity (e.g., Harbitz et al., 2014).

V_a is prone to underestimation because the resolution of bathymetric data and reflection seismic data is typically too low to resolve thin and far travelled turbidites approaching zero thickness in the distal parts, making a clear distinction between V_a and V_t difficult.

Recent studies have shown that processes of basal erosion and incorporation of seafloor material can lead to a significant increase in V_a (Nugraha et al., 2022; Sobiesiak et al., 2018), but this volume does not represent the volume of initial failed landslide material V_e . The deposit in the sink area might therefore not be a good representation and therefore we advocate to consider V_e , $V_{e,r}$, and $V_{e,void}$ to estimate the initial failed volume.

7. Conclusions

In the absence of extensive geological, geotechnical, and age data, the hazard of submarine landslides is oftentimes assessed from their volume. Next to the landslide mechanism, which is difficult to express in quantitative terms, the initial failed volume is an important factor in tsunami simulations (Murty, 2003), for the estimation of which we identify the most robust method. It is not only the data type and quantity that controls the quality of the volume estimation but also the landslide's emplacement mechanism. If no seismic data from the source area of the landslide is available, the initial failed landslide volume V_e can relatively reliably be determined only for frontally unconfined landslides. For unconfined or mixed systems, this approach will underestimate the true initial failed volume because the amount of landslide material that was mobilized but remained inside the source area is neglected. Seismic data are required to estimate the volume of landslide material that remained inside the source area. If such data are not available, we find that the most robust approximation for the initial failed volume of an unconfined or mixed-system submarine landslide also is to determine the amount of evacuated landslide material between the pre-failure and present-day seafloors inside the source area from the void space between both surfaces using bathymetric data.

The initial failed volume has previously been estimated using the seismically identified deposit ($V_{a,bulk}$). It is important to acknowledge that this may be prone to extreme overestimation (more than 200% in this case) because of in situ deformation of sediments underlying the pre-failure seafloor in the sink area that may result from rapid deposition or shearing of the accumulating landslide deposits. When estimating the volume from the amount of seismically chaotic, transparent, or disrupted seismic facies, we advocate for balancing this against the initial failed volume estimated from bathymetric data, which yields a more conservative estimate.

Declarations

Acknowledgements

This work is part of the Deutsche Forschungsgemeinschaft (DFG) – funded TRISCO project (UR 226/3-1) under which Thore F. Sager was employed. We thank Jürgen Grabe (Institute of Geotechnical Engineering & Construction Management, Hamburg University of Technology (TUHH), Hamburg, Germany) for supporting funding acquisition. Many thanks are given to the master and the crew of RRS Charles Darwin who facilitated bathymetric and seismic data acquisition during voyage 178, and Frode Eriksen of VBPR, Oslo for technical support on the same cruise. IHS Markit and Schlumberger provided academic licenses for Kingdom Suite and OMEGA, respectively. We would like to thank an anonymous reviewer and David Tappin (BGS) for reviews and suggestions to improve an earlier version of the manuscript.

Funding (not applicable for MU and CB)

The research leading to results presented in this study received funding from Deutsche Forschungsgemeinschaft (DFG) – TRISCO project Grant Agreement number UR 226/3-1.

Conflicts of Interest/Competing Interests

The authors have no relevant financial or non-financial interests to disclose. These authors have no competing interests to declare that are relevant to the content of this article.

Availability of Datasets and Material

The 3D reflection seismic data from Ana Slide analyzed in the current study are available at the World Data Centre Pangaea repository (<https://doi.pangaea.de/10.1594/PANGAEA.943506>), the 2D reflection seismic data are available under (<https://doi.pangaea.de/10.1594/PANGAEA.943523>), and the multibeam bathymetry data of the study area are available under (<https://doi.pangaea.de/10.1594/PANGAEA.953762>).

Code Availability (Not applicable)

Author Contribution

Conceptualization: TFS, MU, CB; Methodology: TFS; Formal analysis and investigation: TFS; Writing original draft preparation: TFS; Writing – review and editing: TFS, MU, CB; Funding acquisition: MU, CB; Resources: CB; Supervision: MU, CB. TFS produced Figures 1, 2, 3, and 4. All authors reviewed the manuscript.

Additional Declarations for Articles in Life Science Journals that Report the Results of Studies Involving Humans and/or Animals (not applicable)

Ethics Approval (not applicable)

Consent to Participate (not applicable)

Consent for publication (not applicable)

References

1. Berndt, C., Costa, S., Canals, M., Camerlenghi, A., de Mol, B., & Saunders, M. (2012). Repeated slope failure linked to fluid migration: The Ana submarine landslide complex, Eivissa Channel, Western Mediterranean Sea. *Earth and Planetary Science Letters*, *319–320*, 65–74. <https://doi.org/10.1016/j.epsl.2011.11.045>
2. Bondevik, S., Inge Svendsen, J., & Mangerud, J. (1997). Tsunami sedimentary facies deposited by the Storegga tsunami in shallow marine basins and coastal lakes, western Norway. *Sedimentology*, *44*(6), 1115–1131. <https://doi.org/10.1046/j.1365-3091.1997.d01-63.x>
3. Bondevik, S., Løvholt, F., Harbitz, C., Mangerud, J., Dawson, A., & Inge Svendsen, J. (2005). The Storegga Slide tsunami—Comparing field observations with numerical simulations. *Marine and Petroleum Geology*, *22*(1–2), 195–208. <https://doi.org/10.1016/j.marpetgeo.2004.10.003>
4. Camerlenghi, A., Urgeles, R., & Fantoni, L. (2010). A Database on Submarine Landslides of the Mediterranean Sea. In D. C. Mosher, R. C. Shipp, L. Moscardelli, J. D. Chaytor, C. D. P. Baxter, H. J. Lee, & R. Urgeles (Eds.), *Submarine Mass Movements and Their Consequences* (pp. 503–513). Springer Netherlands. https://doi.org/10.1007/978-90-481-3071-9_41
5. Cattaneo, A., Minisini, D., Asioli, A., Canals, M., Lastras, G., Remia, A., Sultan, N., & Taviani, M. (2011). *Age constraints and sediment properties of Ana Slide (Balearic Sea, Western Mediterranean) and implications on age dating of submarine landslides*. 1.
6. Dugan, B. (2012). A Review of Overpressure, Flow Focusing, and Slope Failure. In Y. Yamada, K. Kawamura, K. Ikehara, Y. Ogawa, R. Urgeles, D. Mosher, J. Chaytor, & M. Strasser (Eds.), *Submarine Mass Movements and Their Consequences* (pp. 267–276). Springer Netherlands. https://doi.org/10.1007/978-94-007-2162-3_24
7. Frey Martinez, J., Cartwright, J., & James, D. (2006). Frontally confined versus frontally emergent submarine landslides: A 3D seismic characterisation. *Marine and Petroleum Geology*, *23*(5), 585–604. <https://doi.org/10.1016/j.marpetgeo.2006.04.002>
8. Fruergaard, M., Piasecki, S., Johannessen, P. N., Noe-Nygaard, N., Andersen, T. J., Pejrup, M., & Nielsen, L. H. (2015). Tsunami propagation over a wide, shallow continental shelf caused by the Storegga slide, southeastern North Sea, Denmark. *Geology*, G37151.1. <https://doi.org/10.1130/G37151.1>

9. Gatter, R., Clare, M. A., Kuhlmann, J., & Huhn, K. (2021). Characterisation of weak layers, physical controls on their global distribution and their role in submarine landslide formation. *Earth-Science Reviews*, *223*, 103845. <https://doi.org/10.1016/j.earscirev.2021.103845>
10. Hamilton, E. L. (1979). Sound velocity gradients in marine sediments. *The Journal of the Acoustical Society of America*, *65*(4), 909–922. <https://doi.org/10.1121/1.382594>
11. Harbitz, C. B., Løvholt, F., & Bungum, H. (2014). Submarine landslide tsunamis: How extreme and how likely? *Natural Hazards*, *72*(3), 1341–1374. <https://doi.org/10.1007/s11069-013-0681-3>
12. Haugen, K. B., Løvholt, F., & Harbitz, C. B. (2005). Fundamental mechanisms for tsunami generation by submarine mass flows in idealised geometries. *Marine and Petroleum Geology*, *22*(1–2), 209–217. <https://doi.org/10.1016/j.marpetgeo.2004.10.016>
13. Iglesias, O., Lastras, G., Canals, M., Olabarrieta, M., González, M., Aniel-Quiroga, Í., Otero, L., Durán, R., Amblas, D., Casamor, J. L., Tahchi, E., Tinti, S., & De Mol, B. (2012). The BIG'95 Submarine Landslide-Generated Tsunami: A Numerical Simulation. *The Journal of Geology*, *120*(1), 31–48. <https://doi.org/10.1086/662718>
14. Lafuerza, S., Sultan, N., Canals, M., Lastras, G., Cattaneo, A., Frigola, J., Costa, S., & Berndt, C. (2012). Failure mechanisms of Ana Slide from geotechnical evidence, Eivissa Channel, Western Mediterranean Sea. *Marine Geology*, *307–310*, 1–21. <https://doi.org/10.1016/j.margeo.2012.02.010>
15. Lastras, G., Canals, M., Amblas, D., Ivanov, M., Dennielou, B., Droz, L., Akhmetzhanov, A., & TTR-14 Leg 3 Shipboard Scientific Party. (2006). Eivissa slides, western Mediterranean Sea: Morphology and processes. *Geo-Marine Letters*, *26*(4), 225–233. <https://doi.org/10.1007/s00367-006-0032-4>
16. Lastras, G., Canals, M., Hughes-Clarke, J. E., Moreno, A., De Batist, M., Masson, D. G., & Cochonat, P. (2002). Seafloor imagery from the BIG'95 debris flow, western Mediterranean. *Geology*, *30*(10), 871. [https://doi.org/10.1130/0091-7613\(2002\)030<0871:SIFTBD>2.0.CO;2](https://doi.org/10.1130/0091-7613(2002)030<0871:SIFTBD>2.0.CO;2)
17. Lastras, G., Canals, M., Urgeles, R., Hughes-Clarke, J. E., & Acosta, J. (2004). Shallow slides and pockmark swarms in the Eivissa Channel, western Mediterranean Sea: Shallow slides and pockmark swarms. *Sedimentology*, *51*(4), 837–850. <https://doi.org/10.1111/j.1365-3091.2004.00654.x>
18. Løvholt, F., Bondevik, S., Laberg, J. S., Kim, J., & Boylan, N. (2017). Some giant submarine landslides do not produce large tsunamis: Giant Landslide Tsunamis. *Geophysical Research Letters*, *44*(16), 8463–8472. <https://doi.org/10.1002/2017GL074062>
19. Løvholt, F., Schulten, I., Mosher, D., Harbitz, C., & Krastel, S. (2019). Modelling the 1929 Grand Banks slump and landslide tsunami. *Geological Society, London, Special Publications*, *477*(1), 315–331. <https://doi.org/10.1144/SP477.28>
20. Maslin, M., Owen, M., Day, S., & Long, D. (2004). Linking continental-slope failures and climate change: Testing the clathrate gun hypothesis. *Geology*, *32*(1), 53. <https://doi.org/10.1130/G20114.1>
21. McAdoo, B., Pratson, L., & Orange, D. (2000). Submarine landslide geomorphology, US continental slope. *Marine Geology*, *169*(1–2), 103–136. [https://doi.org/10.1016/S0025-3227\(00\)00050-5](https://doi.org/10.1016/S0025-3227(00)00050-5)
22. Moscardelli, L., & Wood, L. (2015). Morphometry of mass-transport deposits as a predictive tool. *Geological Society of America Bulletin*, *B31221.1*. <https://doi.org/10.1130/B31221.1>

23. Murty, T. S. (2003). Tsunami Wave Height Dependence on Landslide Volume. *Pure and Applied Geophysics*, *160*(10–11), 2147–2153. <https://doi.org/10.1007/s00024-003-2423-z>
24. Nugraha, H. D., Jackson, C. A.-L., Johnson, H. D., Hodgson, D. M., & Clare, M. A. (2022). Extreme erosion by submarine slides. *Geology*, *50*(10), 1130–1134. <https://doi.org/10.1130/G50164.1>
25. Omira, R., Baptista, M. A., Quartau, R., Ramalho, R. S., Kim, J., Ramalho, I., & Rodrigues, A. (2022). How hazardous are tsunamis triggered by small-scale mass-wasting events on volcanic islands? New insights from Madeira – NE Atlantic. *Earth and Planetary Science Letters*, *578*, 117333. <https://doi.org/10.1016/j.epsl.2021.117333>
26. Panieri, G., Camerlenghi, A., Cacho, I., Cervera, C. S., Canals, M., Lafuerza, S., & Herrera, G. (2012). Tracing seafloor methane emissions with benthic foraminifera: Results from the Ana submarine landslide (Eivissa Channel, Western Mediterranean Sea). *Marine Geology*, *291–294*, 97–112. <https://doi.org/10.1016/j.margeo.2011.11.005>
27. Prior, D. B., Bornhold, B. D., & Johns, M. W. (1984). Depositional Characteristics of a Submarine Debris Flow. *The Journal of Geology*, *92*(6), 707–727. <https://doi.org/10.1086/628907>
28. Sager, T. F., Urlaub, M., Kaminski, P., Papenberg, C., Lastras, G., Canals, M., & Berndt, C. (2022). Development and Emplacement of Ana Slide, Eivissa Channel, Western Mediterranean Sea. *Geochemistry, Geophysics, Geosystems*, *23*(11). <https://doi.org/10.1029/2022GC010469>
29. Sobiesiak, M. S., Kneller, B., Alsop, G. I., & Milana, J. P. (2018). Styles of basal interaction beneath mass transport deposits. *Marine and Petroleum Geology*, *98*, 629–639. <https://doi.org/10.1016/j.marpetgeo.2018.08.028>
30. Sun, Q., & Alves, T. (2020). Petrophysics of fine-grained mass-transport deposits: A critical review. *Journal of Asian Earth Sciences*, *192*, 104291. <https://doi.org/10.1016/j.jseaes.2020.104291>
31. Sun, Q., Alves, T. M., Lu, X., Chen, C., & Xie, X. (2018). True Volumes of Slope Failure Estimated From a Quaternary Mass-Transport Deposit in the Northern South China Sea. *Geophysical Research Letters*, *45*(6), 2642–2651. <https://doi.org/10.1002/2017GL076484>
32. Synolakis, C. E., Bardet, J.-P., Borrero, J. C., Davies, H. L., Okal, E. A., Silver, E. A., Sweet, S., & Tappin, D. R. (2002). The slump origin of the 1998 Papua New Guinea Tsunami. *Proceedings of the Royal Society of London. Series A: Mathematical, Physical and Engineering Sciences*, *458*(2020), 763–789. <https://doi.org/10.1098/rspa.2001.0915>
33. Talling, P., Clare, M., Urlaub, M., Pope, E., Hunt, J., & Watt, S. (2014). Large Submarine Landslides on Continental Slopes: Geohazards, Methane Release, and Climate Change. *Oceanography*, *27*(2), 32–45. <https://doi.org/10.5670/oceanog.2014.38>
34. Talling, P. J., Wynn, R. B., Masson, D. G., Frenz, M., Cronin, B. T., Schiebel, R., Akhmetzhanov, A. M., Dallmeier-Tiessen, S., Benetti, S., Weaver, P. P. E., Georgiopoulou, A., Zühlsdorff, C., & Amy, L. A. (2007). Onset of submarine debris flow deposition far from original giant landslide. *Nature*, *450*(7169), 541–544. <https://doi.org/10.1038/nature06313>
35. Vanneste, M., Sultan, N., Garziglia, S., Forsberg, C. F., & L'Heureux, J.-S. (2014). Seafloor instabilities and sediment deformation processes: The need for integrated, multi-disciplinary investigations.

- Marine Geology, 352, 183–214. <https://doi.org/10.1016/j.margeo.2014.01.005>
36. Völker, D. J. (2010). A simple and efficient GIS tool for volume calculations of submarine landslides. *Geo-Marine Letters*, 30(5), 541–547. <https://doi.org/10.1007/s00367-009-0176-0>
37. Watt, S. F. L., Talling, P. J., Vardy, M. E., Masson, D. G., Henstock, T. J., Hühnerbach, V., Minshull, T. A., Urlaub, M., Lebas, E., Le Friant, A., Berndt, C., Crutchley, G. J., & Karstens, J. (2012). Widespread and progressive seafloor-sediment failure following volcanic debris avalanche emplacement: Landslide dynamics and timing offshore Montserrat, Lesser Antilles. *Marine Geology*, 323–325, 69–94. <https://doi.org/10.1016/j.margeo.2012.08.002>
38. Webster, J. M., George, N. P. J., Beaman, R. J., Hill, J., Puga-Bernabéu, Á., Hinestrosa, G., Abbey, E. A., & Daniell, J. J. (2016). Submarine landslides on the Great Barrier Reef shelf edge and upper slope: A mechanism for generating tsunamis on the north-east Australian coast? *Marine Geology*, 371, 120–129. <https://doi.org/10.1016/j.margeo.2015.11.008>
39. Wilson, C. K., Long, D., & Bulat, J. (2004). The morphology, setting and processes of the Afen Slide. *Marine Geology*, 213(1–4), 149–167. <https://doi.org/10.1016/j.margeo.2004.10.005>

Figures

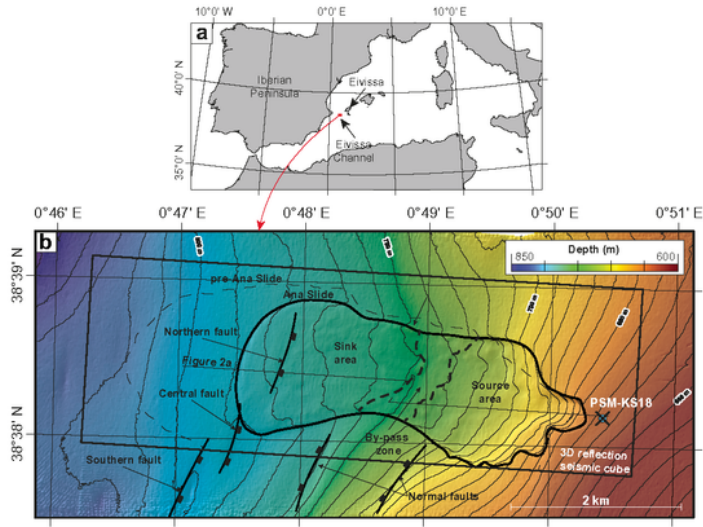


Figure 1

a) Regional map of the western Mediterranean Sea showing the study area in the Eivissa Channel located on the Balearic Promontory between the Iberian Peninsula and the island of Eivissa. **b)** Hillshaded bathymetry map of Ana Slide at water depths between 635 and 790 m. The southern, central, and northern faults comprise a local seafloor antithetic en-echelon fault system that controlled the development of Ana Slide (Sager et al., 2022). The location of Kullenberg gravity core PSM-KS18 is

indicated by a blue symbol ($0^{\circ} 50.453' E$ $38^{\circ} 38.184' N$) presented by Lafuerza et al. (2012). Landslide material involved in Ana Slide was evacuated from the source area and accumulated inside the sink area.

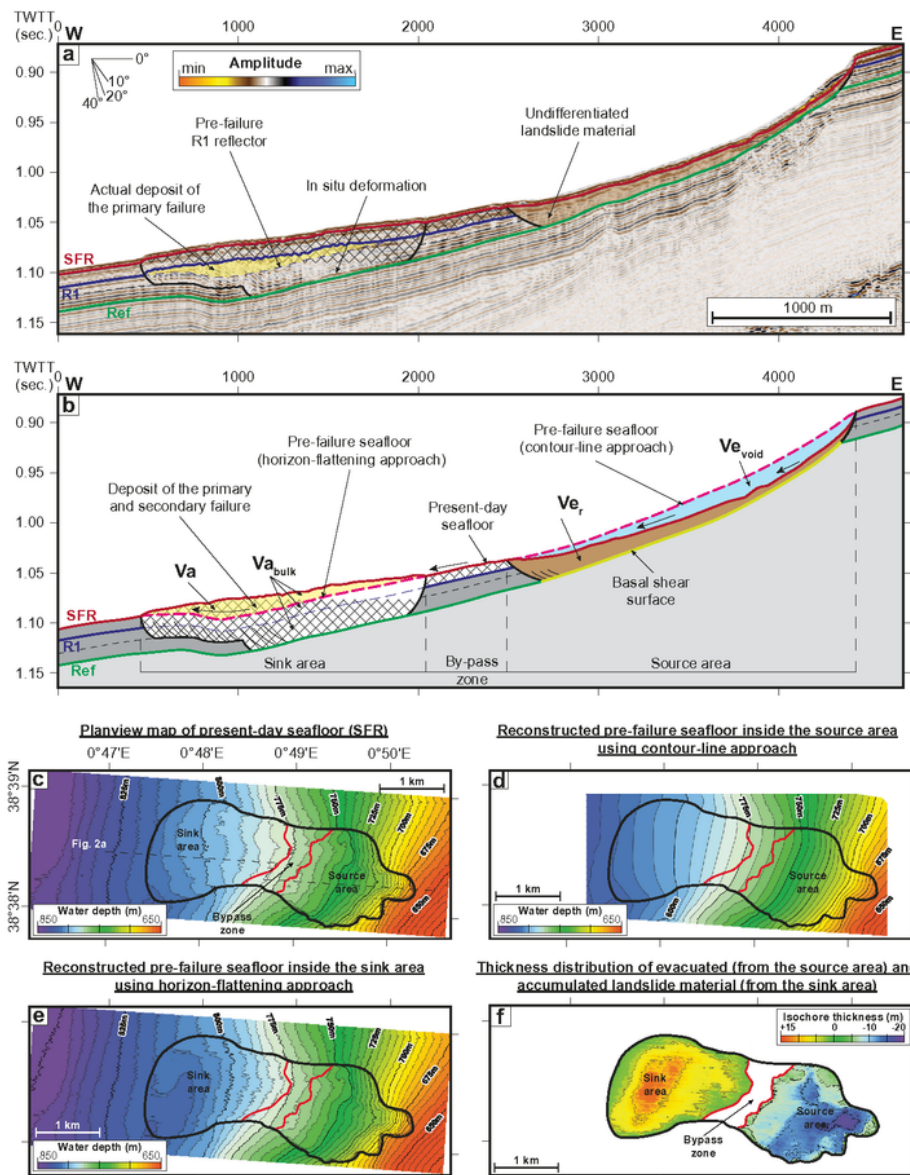


Figure 2

a) Uninterpreted 2D reflection seismic profile (Channel 01 – Line 37) of Ana Slide (see Figure 1) previously presented by Sager et al. (2022). Landslide reflectors Ref (green), R1 (blue), and SFR (red) are

highlighted. **b)** Interpreted profile of Ana Slide showing several volumes related to Ana Slide: V_a describes accumulated landslide material inside the sink area above the pre-failure seafloor. V_{e_r} represents mobilized landslide material (of the primary and secondary failures) which was unable to overcome frontal confinement and ponded downslope inside the source area. $V_{a_{bulk}}$ represents all affected and involved landslide material and slope sediment, while V_a represents the volume of actually accumulated landslide material above the pre-failure seafloor inside the sink area. **c)** Plan-view map of the present-day seafloor SFR reflector mapped from the 3D reflection seismic data. **d)** Reconstructed pre-failure seafloor using the contour-line approach used for volume estimation of $V_{e_{void}}$ inside the source area. **e)** Reconstructed pre-failure seafloor using the horizon-flattening approach for volume estimation of V_a inside the sink area. **f)** Thickness distribution of the reconstructed pre-failure seafloors inside the source (using the contour-line approach) and sink area (using the horizon-flattening approach) and the present-day seafloor SFR. A vertical thickness of up to 20 m of landslide material ($V_{e_{void}}$) was evacuated from the source area, while a thickness of up to 15 m of accumulated landslide material (V_a) was added to the sink area.

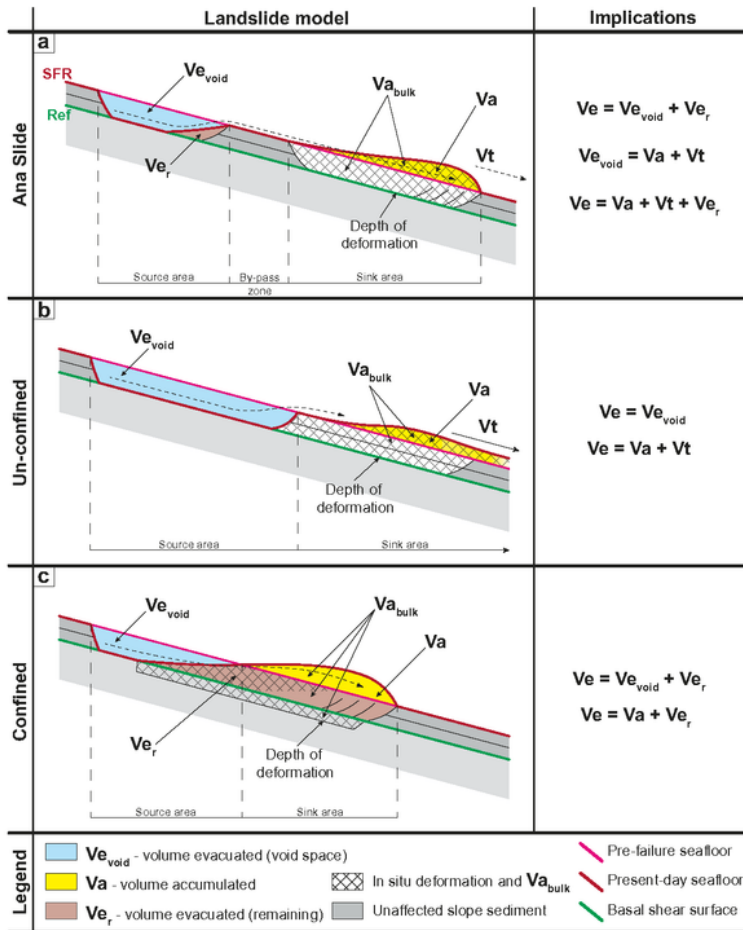


Figure 3

Conceptual models for assessing submarine landslide volume using unconfined and confined slope failure end members. **a)** Model of Ana Slide, with frontal emergence of landslide material above slope sediment that comprises the by-pass zone (in profile) and in situ deformation to a depth of reflector Ref inside the sink area beneath the pre-failure seafloor. **b)** Model of an unconfined landslide with free propagation of landslide material over the seafloor inside of the extensively evacuated source area. **c)**

Model of a confined landslide with restricted propagation of landslide material inside the sink area and limited evacuation of the source area.

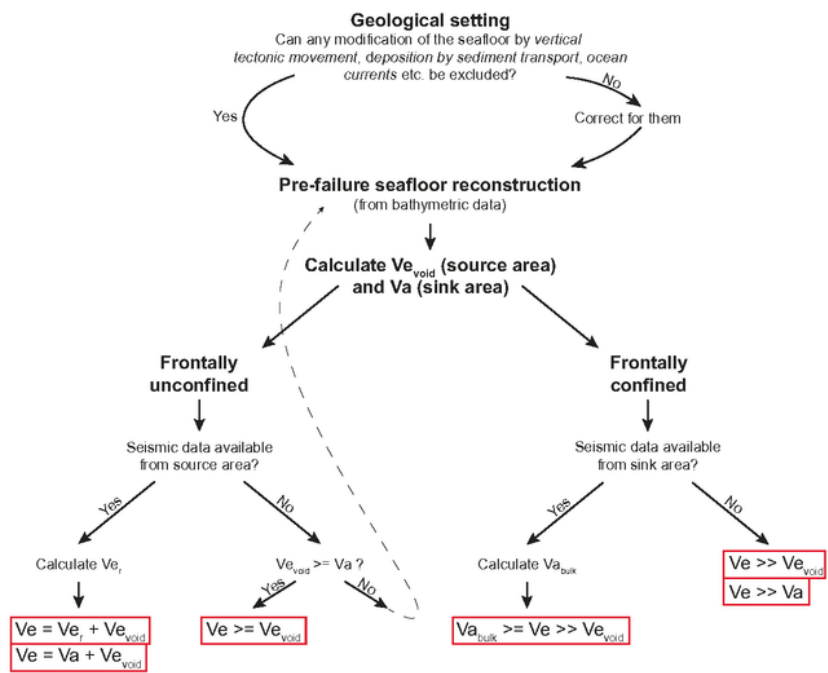


Figure 4

Workflow for assessing volumes of frontally unconfined and confined landslides.

Supplementary Files

This is a list of supplementary files associated with this preprint. Click to download.

- [AssessmentLandslideVolumeSageretalSupplementaryInformation.docx](#)